

QUANTITATIVE FRET MEASUREMENT BASED ON CONFOCAL MICROSCOPY IMAGING AND PARTIAL ACCEPTOR PHOTBLEACHING

XIAO-PING WANG*, HUAL-NA YU[†] and TONG-SHENG CHEN^{†‡}

**Department of Anesthesiology
The First Affiliated Hospital of Jinan University
Guangzhou 510632, P. R. China*

*†MOE Key Laboratory of Laser
Life Science and Institute of Laser Life Science
College of Biophotonics
South China Normal University
Guangzhou 510631, P. R. China
‡chentsh@sncu.edu.cn*

Accepted 5 June 2012
Published 2 August 2012

Fluorescence resonance energy transfer (FRET) technology had been widely used to study protein–protein interactions in living cells. In this study, we developed a ROI-PbFRET method to real-time quantitate the FRET efficiency of FRET construct in living cells by combining the region of interest (ROI) function of confocal microscope and partial acceptor photobleaching. We validated the ROI-PbFRET method using GFPs-based FRET constructs including 18AA and SCAT3, and used it to quantitatively monitor the dynamics of caspase-3 activation in single live cells stably expressing SCAT3 during staurosporine (STS)-induced apoptosis. Our results for the first demonstrate that ROI-PbFRET method is a powerful potential tool for detecting the dynamics of molecular interactions in live cells.

Keywords: Fluorescence resonance energy transfer (FRET); partial acceptor photobleaching; caspase-3; living cells.

1. Introduction

Fluorescence resonance energy transfer (FRET) has become a powerful tool to determine the distances between donor and acceptor fluorophores and molecular conformation variations.¹ Because of its potency, FRET is increasingly used to visualize and

quantify the dynamics of protein–protein interaction in living cells, with high spatio-temporal resolution.² Several FRET methods, including emission ratio method³ and sensitized emission-based method,^{4,5} have been proposed to monitor the dynamics of protein–protein interaction in live cells.

[‡]Corresponding author.

Emission ratio method is a semi-quantitative method for the evaluation of changes in FRET efficiency (E). Sensitized emission-based method is subject to variability because of their strong dependence on external controls for the calibration of FRET efficiency, which introduce a high level of instability to the measure. Most importantly, most of the published correction schemes of sensitized emission-based methods have been implemented on wide-field fluorescence microscope, and the correction is distinctly more complex for confocal images because the sensitivities of the detection channels are varied independently.⁶ On wide-field imaging setups, it suffices to calibrate the setup just once for a given set of filters and fluorophores, and then use it for weeks or months without bothering about it. In contrast, calibrations must be made every time even if identical filter and pinhole settings were used from experiment-to-experiment for confocal FRET imaging. In addition, sensitized emission-based method complicates the experimental design because it requires user to establish co-cultures with donor- and acceptor-expressing cell lines.

The most easily implemented quantitative FRET method is acceptor photobleaching as it does not rely on external references.⁷ There are complete acceptor photobleaching method and partial acceptor photobleaching method. Complete acceptor photobleaching prevents repeated measurements on the same cell⁸ and then it is unsuitable for the dynamics measurement in single live cells. Elder *et al.*⁹ reported a partial acceptor photobleaching FRET method, here named Pa-FRET, by measuring the bleached degree at the acceptor excitation wavelength and donor intensities change at the donor excitation wavelength before and after photobleaching. Our group recently developed another partial acceptor photobleaching FRET method, named Pb-FRET, to quantitatively monitor the FRET efficiency by simultaneously measuring the fluorescence intensities in both donor and acceptor detection channels before and after partial acceptor photobleaching only at donor excitation wavelength.¹⁰ Partial acceptor photobleaching FRET method largely reduces the photodamage to live cells and is not affected by diffusion during photobleaching. Most importantly, partial acceptor photobleaching FRET method is independent of the degree of photobleaching.

Fluorescence confocal microscopy, combined with the availability of genetically encoded fluorescent

proteins, has become a powerful technique for studying molecular interactions inside living cells with improved spatial and temporal resolution, distance range, and sensitivity and a broader range of biological applications.¹¹ The region of interest (ROI) function of fluorescence confocal microscopy combined with partial acceptor photobleaching FRET technique, named ROI-PbFRET, which provide a powerful imaging technique for exploring the molecular interactions in living cells.

The activation of caspase-3 is a central event in the process of apoptosis.¹² To examine the caspase-3 activation by real-time imaging analysis, a FRET plasmid (SCAT3) was constructed, which is composed of ECFP as the FRET donor and Venus as the FRET acceptor, linked by peptides containing the caspase-3 cleavage sequence, DEVD.¹³ The activated caspase-3 cleaves the linker DEVD, and then induces a marked decrease in the FRET efficiency. We recently used emission ratio imaging to qualitatively monitor the dynamics of caspase-3 activation in living cells during anticancer drugs-induced apoptosis.¹⁴

To quantitatively monitor the protein dynamic interaction, we here set up a ROI-PbFRET platform. We validated ROI-PbFRET method by using 18AA construct. We used ROI-PbFRET method to monitor the dynamic activation of caspase-3 in live human lung adenocarcinoma (ASTC-a-1) cells during taurosporine (STS)-induced apoptosis.

2. Materials and Methods

2.1. Materials

TurbofectTM *in vitro* transfection reagent was purchased from Fermentas (USA). Plasmid DNA of 18AA was kindly supplied by Prof. Kaminski.⁹ This construct contains donor (ECFP) and acceptor (enhanced cyan fluorescent protein, EYFP) as well as a linking sequence coding with a short 18AA (amino acid) long polypeptide (GLRSRA-QASNS AVEGSAM) between donor and acceptor. Plasmid DNA of SCAT3 was kindly provided by Dr. Miura.¹³ SCAT3 consists of a donor (enhanced cyan fluorescent protein, ECFP) and an acceptor (Venus, a mutant of yellow fluorescent protein). The donor and the acceptor are linked with a caspase-3 recognition and cleavage sequence (DEVD).^{13,15,16}

2.2. Cell culture and transfection

ASTC-a-1 cells were obtained from the Department of Medicine, Jinan University (Guangzhou, China), and cultured in DMEM (GIBCO) supplemented with 10% fetal calf serum (Sijiqing, Hangzhou, China) in 5% CO₂ at 37°C in a humidified incubator. For transfection, ASTC-a-1 cells were cultured in DMEM supplemented with 10% serum at a density of 4×10^4 cells/ml in 35-mm glass dish. After 24 h, when the cells reached 70–90% confluence in DMEM containing 10% fetal calf serum at 37°C in 5% CO₂, plasmids of 18AA, were transfected into the cells by using Turbofect™ *in vitro* transfection reagent (Fermentas, USA) in 35-mm dish for 24–48 h.

2.3. Two-photon excitation fluorescence lifetime imaging

Fluorescence lifetime measurements were performed as described earlier.¹⁷ Two-photon excitation fluorescence imaging was performed using a Leica TCS SP2 Confocal Laser Scanning Microscope (Leica Microsystems Heidelberg GmbH, Mannheim, Germany). The wavelength of the femtosecond laser was tuned to 800 nm for the excitation of the donor in the cells. Its lifetime was measured using a time-correlate single photon counting (TCSPC) module (SPC-150, Becker and Hickl GmbH, Germany). A bandpass filter was placed in front of the MCP-PMT for detecting fluorescence only from the donor. The FLIM data were processed using the SPCImage software by Becker and Hickl GmbH. Decay curves are analyzed by three exponential fits for 18AA,⁹ while double exponential fits for SCAT3. For FLIM-FRET measurement, the fluorescence lifetime of the donor alone (τ_D) and also in the presence of the acceptor (τ_{DA}) were measured. FRET efficiency can be obtained by $E = 1 - \frac{\tau_{DA}}{\tau_D}$.

2.4. Fitting emission spectral analysis

Spectral images for fitting emission spectral (FES) analysis were acquired as described earlier.¹⁸ Briefly, cells expressed 18AA constructs, SCAT3 were cultured in 96-well flat-bottomed microtiter plates at 5×10^5 per well in PBS. The emission spectra of these plasmids were acquired by auto-microplate reader, respectively. The excitation wavelength of 18AA, (SCAT3) was 418 ± 20 nm and the emission fluorescence was detected by a 470–600 nm bandpass filter.

2.5. Excitation modes

In this study, we defined two excitation modes: D/A-excitation mode and A/D-excitation mode. In the case of D/A-excitation mode, signal from donor is first recorded with the donor excitation, and then the signal from acceptor is recorded with the acceptor excitation; similarly, the A/D-excitation mode means that signal from acceptor is first recorded with the acceptor excitation, and then signal from donor is recorded with the donor excitation.

2.6. Microscope platforms

Both fluorescence imaging and acceptor photobleaching are carried out on Laser Scanning Confocal Microscope system with a $40 \times$ NA 1.3 oil objective (LSM510 Meta, Zeiss, Germany). Donor excitation wavelength is 458 nm. Acceptor excitation wavelength is 514 nm. The acceptor in the chosen region inside the living cells is selectively bleached with the maximum of 514 nm laser line. For Pa-FRET method, CH₁ channel is 475–496 nm, CH₂ channel is 507–529 nm. For Pb-FRET method, CH₁ channel is 475–496 nm, CH₂ channel is LP 560 nm. Both excitation modes are used to measure the FRET efficiency of the same sample and the mean FRET efficiency obtained in both modes is considered to be the actual FRET efficiency. Here, to minimize the effect of photobleaching due to 514 nm excitation and 458 nm excitation before and after photobleaching, the laser intensity used for image acquisition should be as low as possible.

2.7. Statistical analysis

Results are expressed as mean \pm SEM. Data were analyzed by repeated-measures ANOVA with parametric methods and LSD multiple comparison using the statistical software SPSS 10.0 (SPSS, Chicago). Throughout the work, *P* values less than 0.05 were considered to be statistically significant.

3. Results

3.1. FLIM analysis of the FRET efficiency of 18AA

To verify ROI-PbFRET method, we first used FLIM to measure the FRET efficiency of 18AA plasmid in living cells. In our experiments, for the 18AA constructs, it was found that three exponential gave

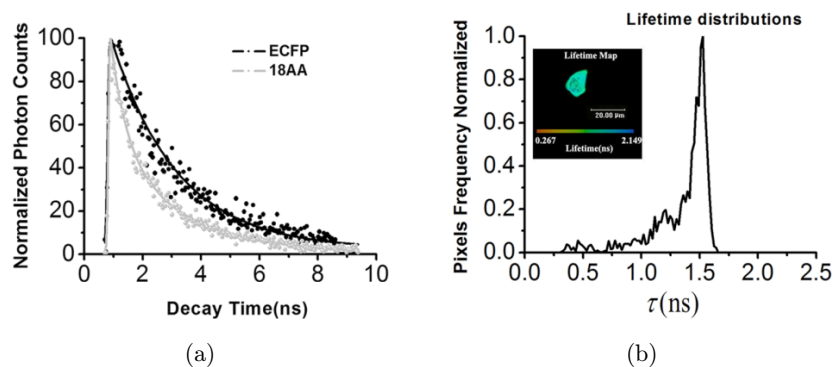


Fig. 1. FLIM analysis of 18AA construct in living cells. (a) ECFP fluorescence lifetime decay curves obtained from single live cells expressing ECFP only and 18AA, respectively. (b) Histograms of the lifetimes of ECFP distribution for the whole cell expressing 18AA. Dashed lines mark the position of the peaks of the lifetime distribution curves. Inset: the corresponding spatial distribution of the mean fluorescence lifetime. Bars: 20 μ M.

the best fits. For the ECFP and SCAT3 constructs, it was found that double exponential gave the best fits. This is in good agreement with previous findings.¹⁹ The fluorescence lifetime decay of ECFP emanating from cells transfected with 18AA was faster than that ECFP alone (Fig. 1(a)), indicating that the 18AA was undergoing FRET. The fluorescent decay constants (τ) of 18AA was 1.49 ± 0.036 ns ($n = 17$), while ECFP was 2.42 ns as reported in our previous publication.¹⁷ Then the FRET efficiency of 18AA was $38.2 \pm 1.5\%$ (Fig. 1(b)).

3.2. FES analysis of the FRET efficiency of 18AA

Spectral imaging (FES) method was used to provide a secondary transfer efficiency measurement for comparison with the results of Pa-FRET and Pb-FRET methods. FES analysis was performed as

described previously.¹⁰ To obtain the FRET efficiency, we need to measure the emission spectra of donor and acceptor. The normalized emission spectra of ECFP or EYFP measured by auto-microplate reader were shown in Fig. 2(a). The emission spectra of 18AA in living cells acquired by auto-microplate reader and the corresponding fitting curve by FES method were shown in Fig. 2(b). The FRET efficiency of 18AA obtained by FES method was $35.7 \pm 1.7\%$.

3.3. Validation of ROI-PbFRET method using 18AA and SCAT3

We next used ROI-PbFRET and Pb-FRET method to measure the FRET efficiency of 18AA in living cells. The fluorescence images of cells expressing 18AA before and after partial acceptor photobleaching in D/A-excitation mode (Left) and

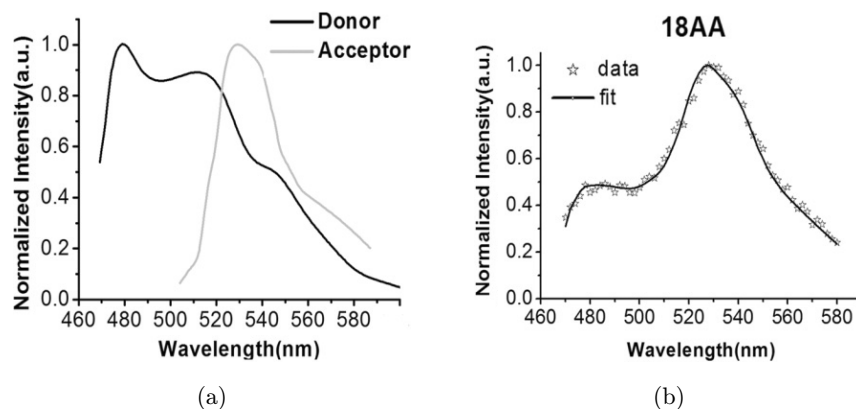


Fig. 2. FES analysis of the FRET efficiency of 18AA plasmid in living cells. (a) Emission spectra of the ECFP only (black curve) and EYFP only (gray curve). (b) Emission spectra of 18AA and the corresponding fitting curves under 398–438 excitation wavelengths. The intensity of the spectra is normalized to one according to maximum value of the spectra.

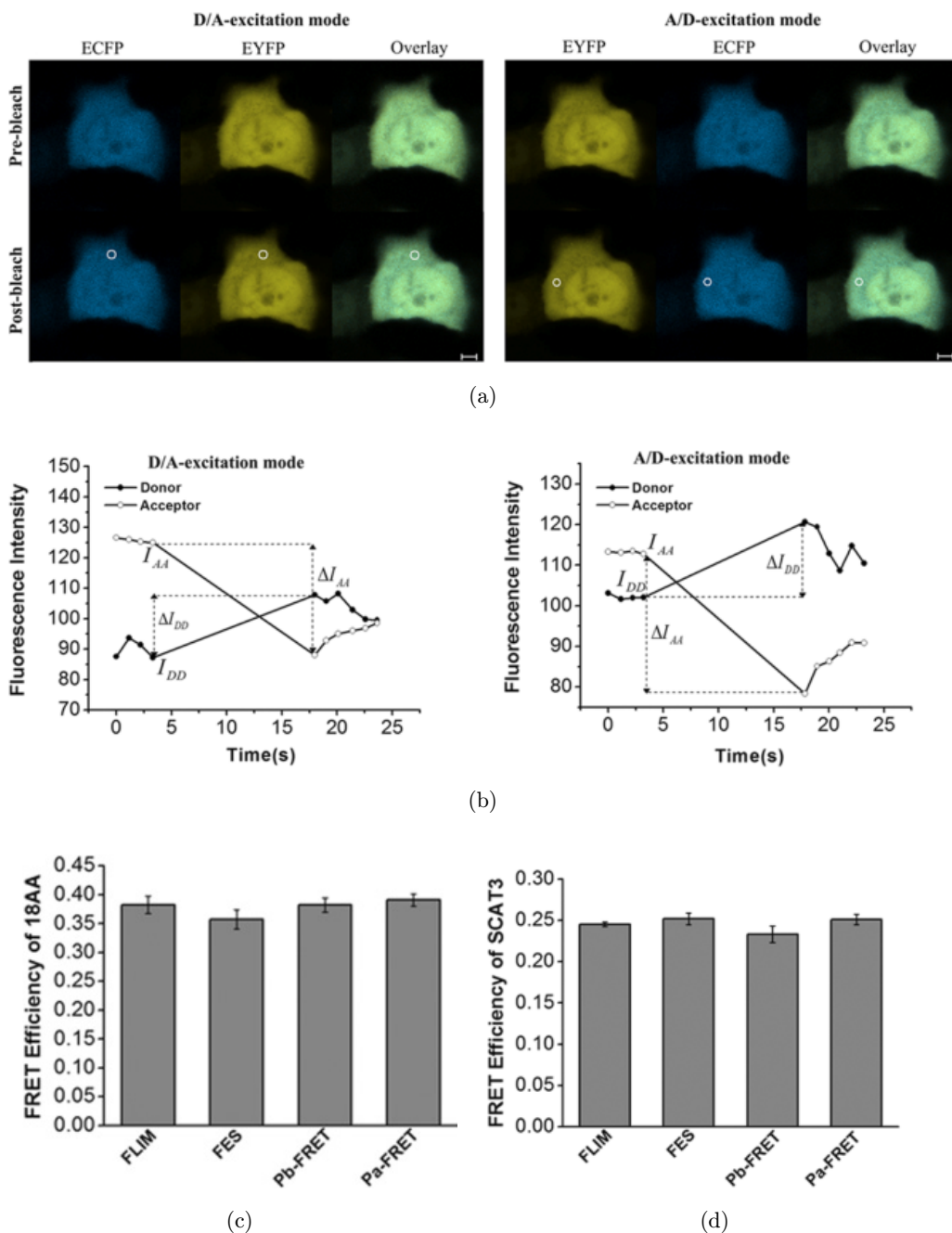


Fig. 3. The FRET efficiencies of 18AA and SCAT3 in living cells by Pa-FRET method. (a) The fluorescence image of cells expressing 18AA from the CH₁ and CH₂ at D/A-excitation mode (Left) and A/D-excitation mode (Right) before (Upper panel) and after (Lower panel) photobleaching. White circles indicate the bleached regions of interest. Scale bar: 5 μ m. (b) The corresponding intensities in the bleached regions of interest. (c) Statistical results of the FRET efficiency of 18AA in living ASTC-a-1 cells obtained by FLIM, FES, Pb-FRET and Pa-FRET methods, respectively. * $P < 0.05$, compared with FLIM; # $P < 0.05$, compared with spectral imaging method. (d) Statistical results of the FRET efficiency of SCAT3 in living ASTC-a-1 cells obtained by FLIM, FES, Pb-FRET and Pa-FRET methods, respectively. * $P < 0.05$, compared with FLIM; # $P < 0.05$, compared with FES.

A/D-excitation mode (Right) were shown in Fig. 3(a), and the corresponding changes of fluorescence intensity in both CH₁ and CH₂ were shown in Fig. 3(b). The statistical result of the FRET efficiency for 18AA from 41 cells in three independent

experiments was $E = 39.1 \pm 1\%$, which was consistent with those detected by FLIM, FES, and Pb-FRET ($38.2 \pm 1.2\%$, $N = 15$) methods, respectively. The statistical result of the FRET efficiency for SCAT3 from 43 cells in three independent experiments by

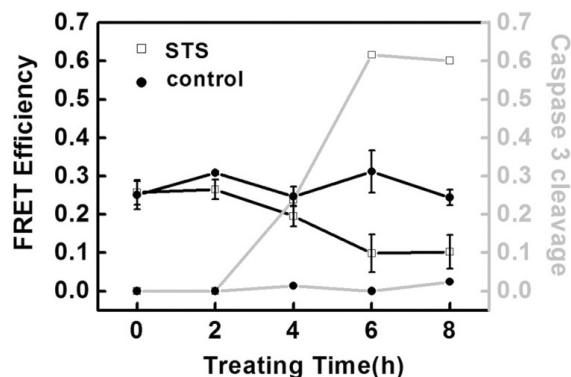


Fig. 4. Temporal profile of the FRET efficiency of SCAT3 (black line) and the degree of caspase-3 activation (gray line) during STS-treated cells. The cells were exposed to $2 \mu\text{M}$ STS (mean \pm SEM).

ROI-PbFRET method was $E = 25.1 \pm 0.6\%$, which was consistent with those detected by FLIM,¹⁷ FES¹⁰ and Pb-FRET methods,¹⁸ respectively (Fig. 3(d)).

3.4. Real-time dynamic analysis of caspase-3 activation in STS-treated cells

We used ROI-PbFRET method to measure the dynamic activation of caspase-3 by real-time quantifying the FRET efficiency of SCAT3 in living cells. The FRET efficiency of the cells expressing SCAT3 after STS treatment and the corresponding degree of caspase-3 activation at 0, 2, 4, 6 and 8 h were shown in Fig. 4 (black line, $N = 8$). After treatment with STS ($2 \mu\text{M}$, time = 0 h), the FRET efficiency of the SCAT3 in living cells remained unchanged for 2 h ($25.77 \pm 3.18\%$ versus $26.48 \pm 2.549\%$). The FRET efficiency of SCAT3 decreased gradually, and reached its minimum at 6 h after STS treatment. In a control experiment, the FRET efficiency of SCAT3 and the corresponding activation degree of caspase-3 at 0, 2, 4, 6 and 8 h were shown in Fig. 4 (gray line, $N = 9$). From the graph, the FRET efficiency of SCAT3-expressing cells remained unchanged throughout the observation period, indicating that the repeated photobleaching did not result in significant changes in FRET efficiency during our time course measurement.

4. Discussion

We here develop a ROI-PbFRET method for real-time monitoring the dynamics of protein–protein interaction in living cells, which oversteps the gap

that the acceptor photobleaching FRET methods are unsuitable for dynamic study in live cells. In our experiments, the degree of photodamage of a ROI photobleaching is about 0.1% to the whole cell and even less for spot photobleaching, making ROI-PbFRET method more suitable for dynamic measurement of molecular interaction.

ROI-PbFRET method can also be used to determine the key optical parameter which is necessary for quantitative measurement of FRET efficiency using sensitized emission-based method such as G factor.^{4,5} The G factor is the loss of donor signal due to FRET with the donor filter set to the increase in acceptor signal due to FRET with the filter set.⁴ The G factor is a constant for a given imaging system and fluorophores. The previous methods used to measure G factor require two reference specimens.²⁰ We can determine the G factor by using the E value obtained by ROI-PbFRET method.

Acceptor photobleaching method is considered to be unsuitable for dynamic application because the photobleaching process can destroy the cells activity. In reality, the area of bleaching to the whole cell was about 0.1%, and the bleaching time is very short in our experiments. Thus, the photodamage of once acceptor ROI photobleaching to the cell can be ignored, making the ROI-PbFRET method become a potential powerful technique for exploring the molecular interaction in living cells.

Contrast to FLIM and spectral imaging method, ROI-PbFRET method is insensitive to autofluorescence and background. It is notable that autofluorescence and background may also interfere with precise measurement of fluorescence lifetime or spectra.²¹ ROI-PbFRET method only relies on the ratio between the increased intensity of donor and the decreased intensity of acceptor, avoiding the disturbance of background signals and autofluorescence. However, the complex photophysical properties in living cells complicate the analysis of FLIM.²² Careful and proper calibration of optical setup and spectral signatures of all participating fluorophores should be considered in spectral imaging method due to high sensitivity to multiple factors, such as considerable amounts of sampling noise, background signals, autofluorescence, and so on.^{21,22} Therefore, ROI-PbFRET method improves the reliability of the measurements in the presence of autofluorescence and background in living cells.

In summary, we set up a ROI-PbFRET method by combining the partial acceptor photobleaching

and the ROI function of confocal microscopy, which can be used to real-time quantitatively monitor the molecular interactions in single live cells.

Acknowledgments

This work is supported by the National Natural Science Foundation of China (NSFC) (Grant 81071491) and Key Project of the Department of Education and Finance of Guangdong Province (cxzd115).

References

1. J. R. Lakowicz, *Principles of Fluorescence Spectroscopy* (Springer Publishing, New York, 2006).
2. A. Masi, R. Cicchi, A. Carloni, F. S. Pavone, A. Arcangeli, "Optical methods in the study of protein-protein interactions," *Adv. Exp. Med. Biol.* **674**, 33–42 (2010).
3. A. Miyawaki, J. Llopis, R. Heim, J. M. McCaffery, J. A. Adams, M. Ikura, R. Y. Tsien, "Fluorescent indicators for Ca²⁺ based on green fluorescent proteins and calmodulin," *Nature* **388**, 882–887 (1997).
4. G. W. Gordon, G. Berry, X. H. Liang, B. Levine, B. Herman, "Quantitative fluorescence resonance energy transfer measurements using fluorescence microscopy," *Biophys. J.* **74**, 2702–2713 (1998).
5. T. Zal, N. R. Gascoigne, "Photobleaching-corrected FRET efficiency imaging of live cells," *Biophys. J.* **86**, 3923–3939 (2004).
6. J. Van Rheenen, M. Langeslag, K. Jalink, "Correcting confocal acquisition to optimize imaging of fluorescence resonance energy transfer by sensitized emission," *Biophys. J.* **86**, 2517–2529 (2004).
7. J. Roszik, J. Szölloosi, G. Vereb, "AccPbFRET: An ImageJ plugin for semi-automatic, fully corrected analysis of acceptor photobleaching FRET images," *BMC Bioinformatics* **19**, 346 (2008).
8. R. N. Day, A. Periasamy, F. Schaefe, "Fluorescence resonance energy transfer microscopy of localized protein interactions in the living cell nucleus," *Methods* **25**, 4–18 (2001).
9. A. D. Elder, A. Domin, G. S. Kaminski Schierle, C. Lindon, J. Pines, A. Esposito, C. F. Kaminski, "A quantitative protocol for dynamic measurements of protein interactions by Förster resonance energy transfer-sensitized fluorescence emission," *J. R. Soc. Interface* **6**, S59–S81 (2009).
10. L. X. Wang, T. S. Chen, J. L. Qu, X. B. Wei, "Photobleaching-based quantitative analysis of fluorescence resonance energy transfer inside single living cell," *J. Fluoresc.* **20**, 27–35 (2010).
11. R. B. Sekar, A. Periasamy, "Fluorescence resonance energy transfer (FRET) microscopy imaging of live cell protein localizations," *J. Cell Biol.* **160**, 629–633 (2003).
12. N. A. Thornberry, Y. Lazebnik, "Caspases: Enemies within," *Science* **281**, 1312–1316 (1998).
13. K. Takemoto, T. Nagai, A. Miyawaki, M. Miura, "Spatio-temporal activation of caspase revealed by indicator that is insensitive to environmental effects," *J. Cell Biol.* **160**, 235–243 (2003).
14. Y. Y. Lu, T. S. Chen, X. P. Wang, L. Li, "Single-cell analysis of dihydroartemisinin-induced apoptosis through reactive oxygen species-mediated caspase-8 activation and mitochondrial pathway in ASTC-a-1 cells using fluorescence imaging techniques," *J. Biomed. Opt.* **15**, 046028-1-16 (2010).
15. Y. H. Wu, C. X. Zhou, L. Y. Song, X. P. Li, S. Y. Shi, J. X. Mo, H. Y. Chen, H. Bai, X. M. Wu, J. Zhao, R. P. Zhang, X. J. Hao, H. D. Sun, Y. Zhao, "Effect of total phenolics from *Laggera alata* on acute and chronic inflammation models," *J. Ethnopharmacol.* **108**, 243–250 (2006).
16. Y. H. Wu, F. Wang, Q. X. Zheng, L. X. Lu, H. T. Yao, C. X. Zhou, X. M. Wu, Y. Zhao, "Hepatoprotective effect of total flavonoids from *Laggera alata* against carbon tetrachloride-induced injury in primary cultured neonatal rat hepatocytes and in rats with hepatic damage," *J. Biomed. Sci.* **13**, 569–578 (2006).
17. W. L. Pan, J. L. Qu, T. S. Chen, L. Sun, J. Qi, "FLIM and emission spectral analysis of caspase-3 activation inside single living cell during anticancer drug-induced cell death," *Eur. Biophys. J.* **38**, 447–456 (2009).
18. L. X. Wang, T. S. Chen, J. L. Qu, X. B. Wei, "Quantitative analysis of caspase-3 activation by fitting fluorescence emission spectra in living cells," *Micron* **40**, 811–820 (2009).
19. M. Millington, G. J. Grindlay, K. Altenbach, R. K. Neely, W. Kolch, M. Bencina, N. D. Read, A. C. Jones, D. T. Dryden, S. W. Magennis, "High-precision FLIM-FRET in fixed and living cells reveals heterogeneity in a simple CFP-YFP fusion protein," *Biophys. Chem.* **127**, 155–164 (2007).
20. H. Chen, H. L. Puhl 3rd, S. V. Koushik, S. S. Vogel, S. R. Ikeda, "Measurement of FRET efficiency and ratio of donor to acceptor concentration in living cells," *Biophys. J.* **91**, L39–L41 (2006).
21. S. Levy, C. D. Wilms, E. Brumer, J. Kahn, L. Pnueli, Y. Arava, J. Eilers, D. Gitler, "SpRET: Highly sensitive and reliable spectral measurement of absolute FRET efficiency," *Microsc. Microanal.* **17**, 176–190 (2011).
22. C. Thaler, S. V. Koushik, P. S. Blank, S. S. Vogel, "Quantitative multiphoton spectral imaging and its use for measuring resonance energy transfer," *Biophys. J.* **89**, 2736–2749 (2005).